Tree Physiology 00, 1–15
https://doi.org/10.1093/treephys/tpac117

Research paper

First evidence of nanoparticle uptake through leaves and roots in beech (*Fagus sylvatica* L.) and pine (*Pinus sylvestris* L.)

Paula Ballikaya[1,2,8], Ivano Brunner[1], Claudia Cocozza[3], Daniel Grolimund[4], Ralf Kaegi[5], Maria Elvira Murazzi[1], Marcus Schaub[1], Leonie C. Schönbeck[1,6], Brian Sinnet[5] and Paolo Cherubini[1,2,7]

[1]WSL Swiss Federal Institute for Forest, Snow and Landscape Research, Zürcherstrasse 111, CH-8903 Birmensdorf, Switzerland; [2]Department of Geography, University of Zurich, Winterthurerstrasse 190, CH-8057 Zurich, Switzerland; [3]Department of Agriculture, Food, Environment and Forestry (DAGRI), University of Florence, Via delle Cascine, 5, I-50145 Florence, Italy; [4]Swiss Light Source, PSI Paul Scherrer Institute, Forschungsstrasse 111, CH-5232 Villigen PSI, Switzerland; [5]Eawag Swiss Federal Institute of Aquatic Science and Technology, Department Process Engineering, Überlandstrasse 133, CH-8600 Dübendorf, Switzerland; [6]Department of Botany & Plant Sciences, University of California Riverside, 2150 Batchelor Hall, Riverside, CA 92521-0124 USA; [7]Department of Forest and Conservation Sciences, Faculty of Forestry, University of British Columbia, 2004-2424 Main Mall, Vancouver, BC V6T 1Z4, Canada; [8]Corresponding author (paula.ballikaya@wsl.ch)

Received May 30, 2022; accepted October 10, 2022; handling Editor Roberto Tognetti

Trees have been used for phytoremediation and as biomonitors of air pollution. However, the mechanisms by which trees mitigate nanoparticle pollution in the environment are still unclear. We investigated whether two important tree species, European beech (*Fagus sylvatica* L.) and Scots pine (*Pinus sylvestris* L.), are able to take up and transport differently charged gold nanoparticles (Au-NPs) into their stem by comparing leaf-to-root and root-to-leaf pathways. Au-NPs were taken up by roots and leaves, and a small fraction was transported to the stem in both species. Au-NPs were transported from leaves to roots but not *vice versa*. Leaf Au uptake was higher in beech than in pine, probably because of the higher stomatal density and wood characteristics of beech. Confocal (3D) analysis confirmed the presence of Au-NPs in trichomes and leaf blade, about 20–30 μm below the leaf surface in beech. Most Au-NPs likely penetrated into the stomatal openings through diffusion of Au-NPs as suggested by the 3D XRF scanning analysis. However, trichomes were probably involved in the uptake and internal immobilization of NPs, besides their ability to retain them on the leaf surface. The surface charge of Au-NPs may have played a role in their adhesion and uptake, but not in their transport to different tree compartments. Stomatal conductance did not influence the uptake of Au-NPs. This is the first study that shows nanoparticle uptake and transport in beech and pine, contributing to a better understanding of the interactions of NPs with different tree species.

Keywords: environmental pollution, leaf and root uptake, stomatal pathway, surface charge, trichomes, woody species.

Introduction

Terrestrial vascular plants have the ability to take up metals, organic contaminants and ultrafine particulate matter (PM), such as nanoparticles (NPs), influencing their environmental fate through bioaccumulation and potential migration into the food chain. Soils are receiving compartments of most NPs, released from sewage sludge and landfills, and from use of agrochemicals with delivery systems based on engineered NPs, such as NP-containing pesticides (Larue et al. 2014, Avellan et al. 2019). Another major source is the atmosphere (Tripathi et al. 2017, Kumar et al. 2018). Metal NPs, such as particulate platinum and lead, can be directly emitted into the atmosphere from human activities and can interact with plants through the leaves when wind-dispersed and deposited on the leaf surface (Uzu et al. 2010, Hong et al. 2014, Kranjc et al. 2018). Atmospheric fallouts of lead-NPs derived from a lead-recycling plant have been found trapped on the leaf surfaces and in the stomatal openings of lettuce leaves

(Uzu et al. 2010). Similarly, the penetration of gold (Au)-NPs via stomatal pathways was demonstrated in plant leaves when simulating the scenario of particles in raindrops falling on plants (Ha et al. 2021).

Different types of NPs (e.g., silver, gold, zinc oxide, titanium dioxide) were used to study the uptake, transport and effects of NPs in plants (Du et al. 2017, Khan et al. 2017, Su et al. 2019, Liu et al. 2020). Au-NPs are commonly used in studies with plant systems because of their low toxicity to plants (e.g., Ma and Quah, 2016) and their physicochemical properties (sizes, shapes and surface charges) that makes them of use in the synthesis of nanoencapsulated nutrients applied in agriculture (Kumar et al. 2018). Au-NPs are not known to have any effect on gas exchange rates, but they can negatively affect vegetative growth and seed germination at high concentrations (up to 25 p.p.m., Arora et al. 2012; 100 to 400 p.p.m., Siddiqi and Husen, 2016) or increase plant growth at low NP concentration (1 μg mL^{-1}, Feichtmeier et al. 2015). Root uptake of Au-NPs was observed under hydroponic conditions (e.g., Judy et al. 2012, Koelmel et al. 2013, Li et al. 2016), and some studies even reported the accumulation of particulate Au in plants in natural environments (Lintern et al. 2013, Luo and Cao, 2018). Nanoparticles can penetrate the cell wall and cell membrane of root epidermis or enter plant leaves via a polar pathway (e.g., trichomes, hydathodes, necrosis spots, stomata) and a nonpolar pathway (i.e., cuticle and its pores) (Avellan et al. 2021). Although there are controversial results on root uptake depending on type of NPs, plant traits and time of exposure (Ma et al. 2010), it is generally accepted that particles >100 nm can be taken up by plant roots despite the size exclusion limits of <20 nm (Ma and Yan, 2018). Nanoparticles can induce the formation of nanoscale membrane holes in the root cells that allow their accumulation in the roots (Zhu et al. 2012) or pass through discontinuous regions in the Casparian band of the root tip known as the crack-entry mode, where the endodermal cells are not yet mature and at the sites of secondary root initiation (Li et al. 2020, Murazzi et al. 2022). Surface charge is also involved in the root uptake and transport of NPs, as it was observed for Au-NPs (Zhu et al. 2012, Koelmel et al. 2013, Li et al. 2016, Ma and Quah, 2016). Stomata seem to be the primary route for the foliar uptake of a large range of NPs (Lv et al. 2019). Eichert et al. (2008) were among the first to confirm the stomatal uptake of water-suspended hydrophilic particles (ranging from 40 nm or 1 μm) in broad bean (*Vicia faba*) and leek (*Allium porrum*). However, the stomatal uptake of NPs is likely dependent on the plant morphology and physiological status (Avellan et al. 2021). Although long-distance transport of various NPs can occur via xylem (from roots to leaves) and via phloem (from leaves to roots), it is still unclear how the NPs cross the plant membrane—through endocytosis or through aquaporins and plasmodesmata channels, and when they move using symplastic pathways (Tripathi et al. 2017). It seems that transport coincides with the solubility of the NPs: the highest leaf–root transport occurs for the most soluble NPs (Schwab et al. 2016). Regardless of their coating and sizes, Avellan et al. (2019) showed that Au-NP transport from leaves to roots in wheat is possible and that Au-NPs <50 nm were exuded into the soil. In the case of root uptake, NPs could clog the vasculature and lead to decreased water fluxes and thus, transpiration, which strongly depends on drought tolerance and plant architecture (Schwab et al. 2016). Whether or not there is a possible influence of the plant gas exchanges (i.e., photosynthesis and stomatal conductance) on the NP uptake and transport is not yet known.

First observations of foliar uptake of airborne ultrafine particles in trees were reported inside *Betula pendula* leaves exposed to the particles at wind speed (Räsänen et al. 2017). However, the presence of NPs in different tree compartments (i.e., leaves, stem and roots) has barely been investigated. Although the ability of trees to trap pollutants on leaf surfaces has been demonstrated (Han et al. 2020), still only few studies were conducted to explore the uptake and transport pathways of NPs in trees. Zhai et al. (2014) reported that Au-NPs can be taken up and transported from hydroponic solution to poplar roots, stems and leaves. The authors found that Au-NPs accumulated in the plasmodesmata of the phloem in root cells suggesting that transport between cells and throughout the whole plant is possible. Similar results were reported by Su et al. (2020) in citrus trees after trunk injection, where transport of silver (Ag)-NPs from the xylem to the phloem was facilitated by steric repulsive interactions between NPs and conducting tube surfaces. Cocozza et al. (2019) found higher Ag concentrations in the stems of different tree species after foliar application than after root application, suggesting phloem transport of Ag-NPs along with photosynthates. However, evidence supporting the phloem transport of NPs after their penetration through stomatal openings and cuticles is still lacking (Lv et al. 2019), and while much is known about NPs in crop plants, the uptake processes of NPs in trees have been barely studied.

In this study, we investigated whether trees are able to take up Au-NPs and transport them into their stem. We compared leaf-to-root with root-to-leaf NP pathways to assess if the difference between NP exposure belowground and aboveground results in different uptake and accumulation patterns in the trees. We used Au-NPs as model NPs because of their chemical stability and ease of synthesis, functionalization and analytical detection. Au-NPs are commonly considered to be stable in aqueous media and resistant to oxidative dissolution under certain experimental conditions (Koelmel et al. 2013). However, complexation of Au to cyanide, hydroxyl and thiol ligands resulting in the dissolution of Au-NPs has been recently documented in freshwater wetland mesocosms (Avellan et al. 2018). It is unlikely that Au-NPs will

have any environmental relevance in future, although they have been particularly used in industrial applications such as optical sensors, targeted drug delivery carriers and cancer therapy agents (Ma and Quah, 2016). The aims of this study were: (i) to assess to what extent Au-NPs are taken up by two widely spread tree species in Europe (European beech (*Fagus sylvatica* L.) and Scots pine (*Pinus sylvestris* L.)) through the roots and leaves and to understand the uptake dynamics, (ii) to investigate the influence of different surface charges (i.e., positive, negative or neutral) on the uptake and transport of Au-NPs in these two tree species, (iii) to gain insights into NP distribution within the leaves and (iv) to determine whether the Au uptake correlates with the trees' gas exchange rates.

Materials and methods

Characterization of Au-NPs

Spherical Au-NP suspensions (1 mg mL^{-1}, 99.99% purity) with primary particle size of 40 ± 5 nm were acquired from NanoComposix Inc. (Zürich, Switzerland). The hydrodynamic diameter and zeta potential of Au-NPs were measured in deionized water and in Hoagland's nutrient solution (Table S1 available as Supplementary data at *Tree Physiology* Online) using dynamic light scattering (Zetasizer ZS, Malvern Panalytical Ltd, UK). The Au-NPs were functionalized with branched polyethylenimine (BPEI), carboxyl (lipoic acid) and polyethylene glycol (PEG), resulting in positive (Au(+)), negative (Au(−)) and neutral (Au(0)) surface charges of the Au-NPs, respectively. Details about the Au-NP properties are described in the Supplementary data (see Section S2 and Table S1 available as Supplementary data at *Tree Physiology* Online).

Plant material and growth conditions

Two-year-old seedlings (144 in total) of Scots pine (*P. sylvestris*) and European beech (*F. sylvatica*) from Emme-Forstbaumschulen AG (Wiler bei Utzenstorf, Switzerland) were planted in the nursery at WSL (Birmensdorf, Switzerland) (47°21′16″ N, 8°26′16″ E; 518 m a.s.l.). The plants were grown in a sand-agricultural soil substrate (1:1) in 4 L plastic pots (18.5 cm × 22 cm) from March to June 2019. The sand was included in the substrate to improve aeration and promote the development of fine roots, as well as to facilitate the transplanting for the hydroponic part of the experiment. The seedlings were watered regularly to avoid reduced soil-water content and no fertilizer was applied. At the end of June 2019, healthy, growing trees were selected for NP exposure. The experimental layout was a randomized block design with nine replicates for the two species and four treatments (Au(+), Au(−), Au(0) and control) for the root and leaf applications. During the experiment, three harvests were planned where three individuals per species and treatment would be harvested.

Nanoparticle application

Preparation of NP stock suspensions A quarter-strength Hoagland's solution was prepared according to the procedure of Hoagland and Arnon (1950). Detailed components and concentration of the Hoagland's solution are listed in Table S2 available as Supplementary data at *Tree Physiology* Online. Chemicals such as KNO_3 (99.0%), $Ca(NO_3)_2{*}4H_2O$ (98.5%), $MgSO_4{*}7H_2O$ (99.5%) and $(NH_4)2HPO_4$ (97.0%) were selected as main macronutrients for the plants' 24 h treatment (in hydroponic conditions).

A 100 mL stock solution of each macronutrient was prepared separately and autoclaved at 120 °C for 20 min. Finally, the nutrient stock solutions were cooled under vacuum to room temperature and kept at 4 °C until use. On the day of the application, all Hoagland components were combined in ultrapure water to obtain the final nutrient solution. Ultrapure water was produced by a Milli-Q® water system from Merck Millipore (Darmstadt, Germany).

Au(+), Au(−) and Au(0) NP stock suspensions were prepared in a quarter-strength Hoagland's solution at a concentration of 500 μg L^{-1} for the root and leaf applications. The obtained Au-NP suspensions were dispersed by ultrasonication in a water bath for 5 min (100% power; Elmasonic P 180 H, Elma®, Singen, Germany). The initial pH of the stock suspensions were between 5.5 and 6.0.

Root application On the day of the exposure, trees were carefully removed from the soil and roots were thoroughly washed first under tap water to remove all adhering soil particles and then under deionized water to remove further impurities. The three Au-NP treatments (Au(+), Au(−), Au(0) NPs) were performed by exposing the roots of trees (n = 9) under hydroponic conditions into a 250 mL graduated cylinder filled with 200 mL Au-NP suspension for 24 h (Figure 1A), allowing higher availability of Au-NPs to the plants than if trees were in soil (Wojcieszek et al. 2020). During the treatment, the Au-NP suspensions were neither replaced nor refilled. Control trees were transplanted following the same procedure as described above and arranged in quarter-strength Hoagland's solution only. After 24 h, Au NP-treated and control trees were replanted in their respective pots in the same soil, without rinsing the roots.

Leaf application Abaxial and adaxial foliar surfaces of selected pine and beech trees (n = 9) were sprayed with Au(+), Au(−) and Au(0) NPs in suspension using a hand-held sprayer bottle (Figure 1B). The exposure was conducted in a separate chamber to avoid any exposure to the control trees. Each Au-NP treatment consisted of 5–6.5 mL solution (Table S3 available as Supplementary data at *Tree Physiology* Online), sprayed evenly on the foliage of each tree. The foliage was sprayed twice a day for 2 days. This helped to 'slowly' apply the solution to avoid large leaching and also increased

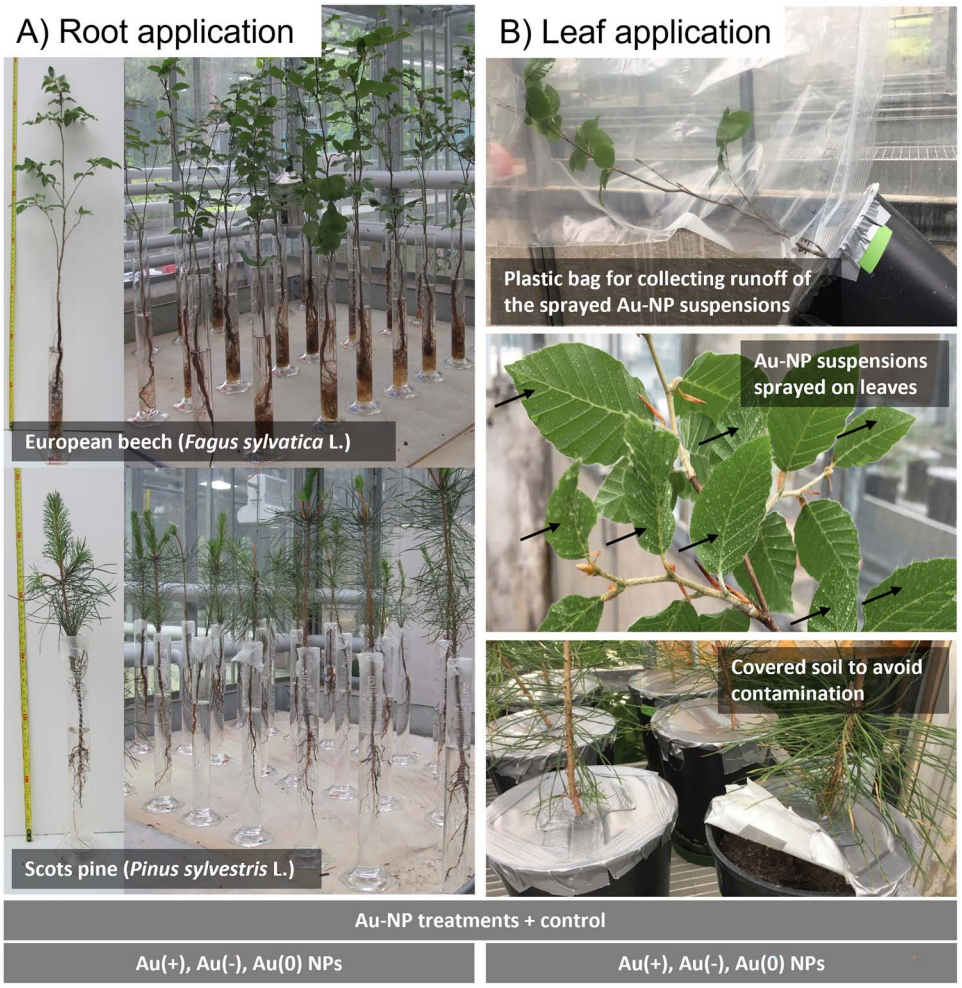

Figure 1. Experimental layout. Au-NP treatments (Au(+), Au(−), Au(0) NPs) and control in the (A) root and (B) leaf application experiments for *F. sylvatica* and *P. sylvestris*.

the chance of NPs to penetrate the leaves by rewetting the leaf surface with NP suspension (Avellan et al. 2021). Parafilm® was used to cover the soil surfaces to prevent unintended Au-NP deposition on the soils (Figure 1B). Trees were left in the greenhouse for 60 days, with two intermediate physiological measurements and harvests, described below. For more details see Section S1.1 in the Supplementary data available at *Tree Physiology* Online.

Gas exchange measurements

During the experiment, gas exchange of randomly selected leaves and needles was measured using a portable photosynthesis system (LI-COR 6800, Lincoln, NE, USA) with a Multiphase Flash™ Fluorometer. Measurements were conducted before the Au-NP exposure on all trees and 20, 40 and 60 days after the Au-NP treatments on a subselection of the trees, which would afterwards be harvested. Greenhouse conditions were kept as stable as possible; plants were maintained at 25/20 °C day/night temperature and 50/85% day/night relative humidity. Photosynthetic active radiation was maintained at 1400 μmol m^{-2} s^{-1}, the flow rate at 500 μmol s^{-1}, air temperature at 25 °C and ambient CO_2 concentration in the chamber at 400 μmol mol^{-1}. The vapor pressure deficit at leaf temperature was set at 1.5 kPa. One uppermost fully expanded beech leaf was selected and clamped into a 6 cm^2 cuvette. In the case of Scots pine, approximately five to six needles were positioned in a flat plane in the cuvette. After ∼15 min of acclimation of the leaf in the cuvette, photosynthesis and stomatal conductance (g_s) were recorded by logging three times within 1 min. For the pines, pictures of the measured needles were taken and the projected leaf area was measured using ImageJ analysis software (Serrano et al. 1997, Renninger et al. 2015).

Sample preparation and measurement of Au concentration

Harvest of trees Leaves, branches, stems and roots of three plants per treatment were harvested and washed with deionized water 20, 40 and 60 days after the Au-NP treatments. For more details see Section S1.2 in the Supplementary data available at *Tree Physiology* Online. The bark was carefully removed from

the stem using a scalpel to avoid possible contamination of the stem measurements from Au-NPs adhering to the bark. However, we cannot exclude possible uptake by the bark during the experiment due to bark deposition. We measured the Au concentration in the middle part of the stem and in the fine roots because they had a higher surface area than the coarse roots and thus highest direct contact with the Au-NPs in the hydroponic system. Samples were immediately frozen in liquid nitrogen and stored at −20 °C until oven-dried at 105 °C for 24 h. Total dry biomass weight (DW, mg) of leaves, roots and stems was determined (DW after 20 days is shown in Figure S3 available as Supplementary data at *Tree Physiology* Online).

Sample preparation for inductively coupled plasma mass spectrometry measurement Dry leaf, stem and fine root material were ground in a ball mill (frequency 30 Hz, 1–2 min; MM400, Retsch) to obtain a homogenized powder. Total digestion of 100 mg of material was conducted in aqua regia (3:1 acid, 9 mL of HCl and 3 mL of HNO_3, Acids Supra Quality, Roth AG, Switzerland) at 200 °C for 15 min and the digests were filled to 50 mL using ultrapure water. Gold concentrations were quantitatively determined by an inductively coupled plasma (ICP)-mass spectrometry (MS) system (Agilent 8900 ICP-MS, Agilent Technologies, Inc., USA), along with blanks and reference materials. As suitable reference materials for measuring Au-NPs in plant tissue were not available yet (Judy et al. 2012, Koelmel et al. 2013), leaves and wood powder of *F. sylvatica* were spiked with Au-NP suspensions to reach a target concentration of 10 p.p.m. Au. This material was then used for quality control. For more details about the preparation of our Au-NP 'reference material' and validation of the digestion method see Section S1.3 of the Supplementary data available at *Tree Physiology* Online.

Samples were measured on an Agilent 8900 against an external calibration series from 0.05 to 2 p.p.b. of a Gold ICP standard (TraceCERT, Sigma Aldrich, Switzerland) prepared in 2% HCl (Supra Quality from Roth AG, Switzerland) on the same day as samples were digested. All samples and controls were adjusted during the measurement against Lutetium (TraceCERT, Sigma Aldrich, Switzerland) as the internal standard. As quality control, a certified sample containing gold (CCB-2 from Inorganic Ventures Inc., USA) was also prepared on the same day as the digests and was measured along with every batch of samples.

2D XRF scanning and 3D chemical tomography imaging

The spatial distribution (on the leaf surface and internal tissues) of Au-NPs on a beech leaf sample was investigated employing the 2D and 3D chemical imaging capabilities of the microXAS beamline at the Swiss Light Source of the Paul-Scherrer-Institute (Villigen, Switzerland). The microXAS beamline corresponds to a versatile, in-vacuum undulator-based hard X-ray microprobe facility devoted to high-resolution multimodal chemical imaging based on X-ray fluorescence (XRF), X-ray spectroscopy (XAS) and X-ray diffraction (XRD) techniques. In the present case, the location of Au-NPs was traced down based on spatially resolved Au fluorescence analysis.

The monochromatic excitation radiation is produced using a fixed-exit, cryo-cooled double-crystal monochromator with the Si(111) crystal pair selected. The energy calibration was performed using an Au foil. The spot size of the monochromatic beam at the sample was dynamically tuned to up to 1 μm × 1 μm by a Kirkpatrick–Baez (KB) mirror system. Flux after focusing (I0) and transmitted intensities were recorded using a micro ionization chamber and a silicon carbide diode, respectively, allowing the analysis of absorption contrast simultaneously together with the XRF signal.

The XRF emitted by the sample was measured for each individual pixel using multiple single-element Si-drift diode detectors (KETEK GmbH, Germany). XRF spectra recorded were deconvoluted employing the PyMca software (Solé et al. 2007). In order to strengthen the robustness of the XRF analysis with respect to potential spectral inferences, all three Au L-edge were excited giving access to multiple Au emission lines. The energy of the excitation beam was 14.6 keV. To validate the Au trace analysis by spectral deconvolution, as an alternative analytical strategy, the local Au concentrations were reconstructed using the edge contrast at the Au L_3-edge. The difference of two micro-XRF maps, recorded below (11.9 eV) and above (12.0 eV) the Au L_3-edge, showed consistently a convincing agreement with chemical images of Au obtained by spectral deconvolution.

A thawed fresh beech leaf (10 × 9 mm^2) was fixed on a frame support as pseudo free-standing object without any additional treatment or preparation. For the identical leaf, 2D chemical imaging (projection along leaf surface normal), as well as 3D chemical tomography based on confocal microscopy, were conducted during two intermittent beamtimes. Accordingly, the chemical tomography data were recorded with the leaf being in dehydrated state. This methodology enabled us to analyze such complex systems in a truly undisturbed manner since any physical slicing or sectioning could easily dislocate the Au-NPs. The analysis was made with prime focus on beech leaves because the concentration of Au-NPs in leaves was higher in beech than in pine. However, analysis of pine needle samples can be performed in a similar manner by confocal XRF microscopy or even by XRF-based computed chemical tomography.

The confocal X-ray microscopy was implemented by constraining the acceptance of one SDD detector by a polycapillary X-ray half-lens with an input focal spot size of <7 μm (XOS, USA). With respect to the leaf surface, the confocal volume was $\sim 2 \times 5 \times 5$ μm^3.

For all 2D and 3D imaging the data were acquired by regular orthogonal grid scanning, however the first scan dimension was scanned in continuous 'on-the fly' mode, reducing overhead time considerably. Typical dwell times per pixel and voxel were 200 ms. Effective spatial resolution was generally given by the chosen pixel or voxel sizes which were scaled based on the given field of view of an image.

Statistical analysis

The reported data show means of three replicates per harvest ± the standard error (SE). Separate analyses were done for the leaf application and root application of the Au-NPs. A two-way analysis of variance (ANOVA) was performed to first assess the differences in Au concentration between the different organs (root, stem, leaf) and treatments (Au(+), Au(−), Au(0) NPs) 20 days after treatments, and then to assess the differences in Au content between different time points (20, 40, 60 days after the treatments) and Au-NP treatments. Pair-wise differences were then analyzed using Fisher LSD test. The relation between g_s and Au concentration in leaves and roots in the leaf and root application, respectively, was tested using Pearson correlation test. Then, differences in the Au concentrations between beech and pine for the leaf and root application 20 days after treatments were tested using the non-parametric Levene *t*-test. Statistical analyses were performed using the OriginPro Version 2021 (OriginLab Corporation, Northampton, MA, USA) scientific data analysis and graphing software. In all cases the statistical significance was based on a *P*-value <0.05.

Results

Au content in plant tissues

The concentration of Au (mg kg^{-1}; Figure 2) 20 days after the Au-NP treatments varied among plant organs in beech and pine. The total Au concentration measured in the roots and in the leaves is derived from Au-NP internalization in the roots/leaves and physical adsorption onto the root/leaf surface after the root and leaf application methods, respectively. Given the chemical stability of Au-NPs, we presume that the measured Au is in the form of Au-NPs. Significant differences ($P < 0.05$) in Au concentration were found between all plant organs (leaves, stem and roots) and treatments (Au(+), Au(−), Au(0) NPs) and their interactions within a tree species (Table 1). Au concentrations detected in leaves, stem and roots were significantly higher ($P < 0.001$) in beech than in pine in the leaf application, but not in the root application (Table 1).

In the root application, a higher concentration of gold was measured in the roots than in the stem (close to the detection limit (DL)) in both species, whereas no Au was found in the leaves (Figure 2A). In roots of beech, the Au concentration in the Au(0) treatment was significantly lower ($P = 0.014$) than in the Au(+) treatment. In pine, the gold concentration in the roots differed significantly ($P < 0.001$) among all Au-NPs treatments, with the trend as follows: Au(−) > Au(+) > Au(0). In the leaf application, Au was found in high concentrations in the leaves and low concentrations in the stem and in the roots (Figure 2B), close to or below the detection limits (0.005–0.01 $\mu g\ kg^{-1}$). In pine, Au (+) treatment resulted in significantly higher ($P < 0.001$) concentrations than Au(−) and Au(0) treatments. A low concentration (0.027 mg kg^{-1}) of Au was detected on the leaves of one control pine tree, which is most likely related to a contamination during handling or analysis. Statistically, no significant difference in the Au concentration in the stem was found among different Au-NP treatments within each species, neither in the leaf nor in the root application. Nevertheless, Au(−) in the stem of the leaf application in beech was significantly higher than the one in the root application.

After 40 and 60 days, gold concentrations measured in other organs than the ones where it was applied were too close to or below the method DL to allow the identification of clear trends (data not shown). Thus, we only considered the Au measured in the leaves and roots over time of the leaf and root application, respectively, to understand the uptake dynamics of Au-NPs at different time points. Leaf and root biomass increased over time (from 20 to 60 days) in both tree species (Figure S4 available as Supplementary data at *Tree Physiology* Online), thus we calculated the absolute Au masses in leaves and roots expressed in milligrams (Figure 3). Significant differences in the Au content were related to time in beech and to the different treatments in pine (Table 2).

As shown in Figure 3A of the root application, the lowest Au content in beech was found in Au(0) at 20 days and in Au(+) at 40 days, whereas in pine, Au content at 20 and 60 days accumulated in the roots to the greatest extent in Au(−). In the leaf application (Figure 3B), the total Au content in beech leaves significantly ($P = 0.035$) increased from 20 to 40 days in Au(−) and from 20 to 60 days in Au(0). No differences in Au content were found among treatments in beech, whereas in pine Au content in Au(+) and Au(−) significantly ($P = 0.014$) differed at 40 days, with Au(+) > Au(−).

Relation between stomatal conductance and Au-NPs

No correlation was found 20 days after the treatments between the g_s and the Au concentration in neither application methods. Nevertheless, the Au concentration in the Au-NP treated trees of the root application appeared to be negatively correlated to g_s, independent of the surface charge (Figure 4). With increasing g_s, total Au concentration significantly decreased in beech after 40 ($r = -0.83$, $P < 0.01$) and 60 days ($r = -0.72$, $P < 0.05$) and in pine after 40 days ($r = -0.66$, $P < 0.05$) of the Au-NP treatments. Measurements of g_s are presented in Figures S4 and S5 available as Supplementary data at *Tree Physiology* Online.

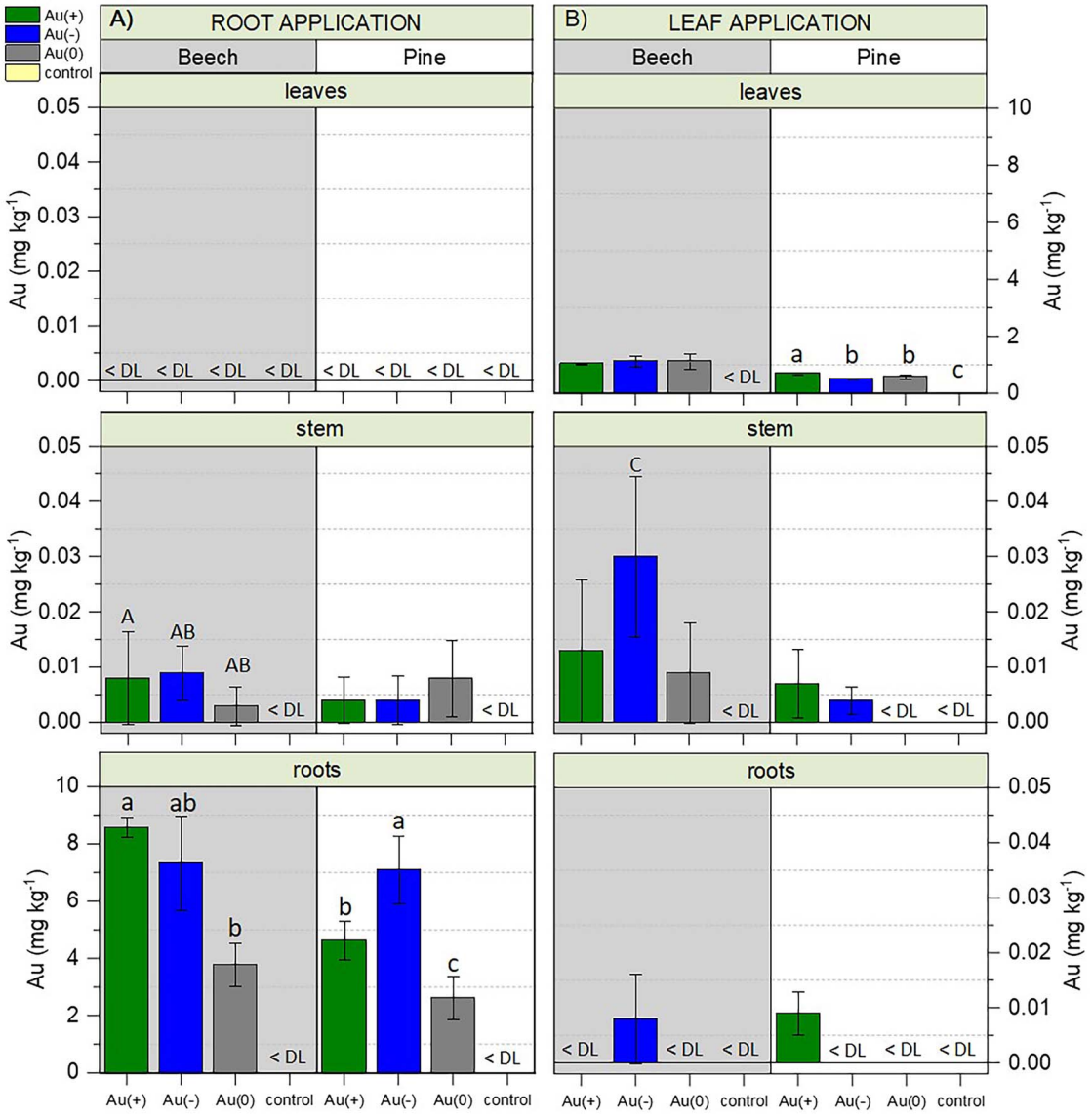

Figure 2. Gold concentrations in leaves, stem and roots in the root (A) and the leaf (B) application 20 days after the treatments. Values below the detection limit (DL) are indicated by '<DL'. Data show the means ± SE ($n = 3$). The lowercase letters stand for statistical differences between organs and treatment groups within a species at $P < 0.05$. The capital letters stand for statistical differences between Au in stem and application groups within a species at $P < 0.05$.

Au-NP distribution in leaf and petiole by 2D XRF scanning and 3D chemical tomography

The hierarchical two-dimensional chemical imaging of a beech leaf revealed Au hotspots sparsely distributed over the entire scanned part of the leaf (10 × 9 mm^2). In general, a rather random distribution is observed (Figure S6, S7, and S8 available as Supplementary Data at *Tree Physiology* Online). However, certain areas showed a higher local density of isolated Au hotspots. Furthermore, zoom-in scans with higher spatial resolution revealed a pronounced spatially correlated distribution (Figure 5). The Au hotspots showed a characteristic size and Au intensity distribution. The size was consistently smaller than the beam size (<1 μm) and the Au intensity in individual hot spots was rather constant. These observations together with the observed magnitude of Au fluorescence in each hotspot point toward the gold still being in particulate form in or on the leaf (along the midrib and lateral veins; Figure 5B, and C) and petiole (Figure 5A) of beech.

Corresponding measurements by confocal X-ray microscopy localized the vast majority of Au either on the leaf surface or associated with trichomes (Figure 6B). However, even within the microscopic volume fraction analyzed by chemical tomography, a gold NP was localized inside the leaf blade.

Table 1. ANOVA two-way results of differences in Au concentrations 20 days after the treatment, between treatments (Au(+), Au(−), Au(0) NPs) and organs (leaf, stem, roots), in leaf and root application, respectively, within a species. Levene *t*-test results of differences in the Au concentrations between beech and pine for the leaf and root application 20 days after the treatments are shown. Significant differences and interactions among variables are indicated: '***' $P < 0.001$, '**' $P < 0.01$, '*' $P < 0.05$.

	Root application						Leaf application					
	BEECH						**BEECH**					
	DF	Sum of squares	Mean square	*F* value	*P* value		DF	Sum of squares	Mean square	*F* value	*P* value	
Treatment	2	12.38	6.19	5.41	0.014	*	2	0.006	0.003	0.09	0.91	
Organs	2	258.62	129.31	113.02	6.45E-11	***	2	7.14	3.57	96.71	2.35E-10	***
Interaction	4	24.68	6.17	5.39	0.004	**	4	0.01	0.002	0.07	0.989	
	PINE						**PINE**					
Treatment	2	9.32	4.66	6.52	0.008	**	2	0.02	0.01	3.69	0.045	*
Organs	2	123.43	61.71	86.30	1.25E-9	***	2	2.26	1.13	442.84	4.93E-16	***
Interaction	4	17.52	4.39	6.13	0.003	**	4	0.03	0.008	3.06	0.043	*
Levene's test	1	7.76	7.76	2.74	0.103		**Levene's test**	1	0.06	0.60	17.31	1.18E-14	***

Table 2. ANOVA two-way results of the total leaf and root Au content between different time points (20, 40, 60 days after the Au-NP treatments) and Au-NP treatments (Au(+), Au(−), Au(0) NPs) in leaf and root application, respectively, within a species. Significant differences and interactions among variables are indicated: '**' $P < 0.01$, '*' $P < 0.05$.

	Root application						Leaf application					
	BEECH						**BEECH**					
	DF	Sum of squares	Mean square	*F*-value	*P*-value		DF	Sum of squares	Mean square	*F*-value	*P*-value	
Time	2	3.48E-6	1.74E-5	7.31	0.004	**	2	1.18E-6	5.91E-7	4.02	0.035	*
Treatment	2	5.68E-5	2.84E-6	1.19	0.325		2	1.24E-7	6.20E-8	0.42	0.661	
Interaction	4	5.35E-5	1.33E-5	5.62	0.004	**	4	8.99E-7	2.24E-7	1.52	0.235	
	PINE						**PINE**					
Time	2	3.97E-7	1.99E-7	3.03	0.073		2	1.22E-6	6.11E-7	2.75	0.099	
Treatment	2	1.24E-6	6.21E-7	9.49	0.0015	**	2	2.42E-6	1.21E-6	5.45	0.014	*
Interaction	4	6.71E-8	1.67E-8	0.25	0.901		4	5.32E-7	1.33E-7	0.59	0.667	

Discussion

Gold in plant organs

Root application The highest concentrations of gold were found in the roots and only a low Au concentration was found in the stems, whereas gold was not detected in the leaves (Figure 2A). Similar results were also reported by Cocozza et al. (2019). In contrast, Zhai et al. (2014) reported the transport of 50 nm particulate Au in woody poplar plants from hydroponic solution to roots, stem and leaves through plasmodesmata. We presume that most of the Au-NPs adhered to the epidermal surface of the roots, which agrees with previous studies reporting that the majority of NPs applied to roots adsorb on their surfaces acting as a sink of NPs (Su et al. 2020). Taylor et al. (2014) found that alfalfa plants respond to gold exposure by down-regulating specific metal transporters to reduce gold uptake through roots. Therefore, the root uptake of a small fraction of Au-NPs may have been promoted by crack-entry mode at or during the application time, root hairs, membrane holes induced by the NPs or mechanical injuries when handling the roots of the root-treated trees, before and after the Au-NP root application. Despite the fact that roots can mainly act as a sink of NPs (Su et al. 2020), low amounts of Au-NPs were still transported upwards through the xylem in the stem (Figure 2A).

Concentrations of Au in the roots were generally observed to decrease from 20 to 60 days after the Au-NP root application (Figure 3), either due to excretion of the Au-NP into the soil or to gradual upward transport, which we were not able to confirm with this experiment. Roots were not washed when transferred from the hydroponic solution to the soil, thus Au-NP uptake could have still occurred after the application time, as probably is the case for the Au(0) treatment in beech.

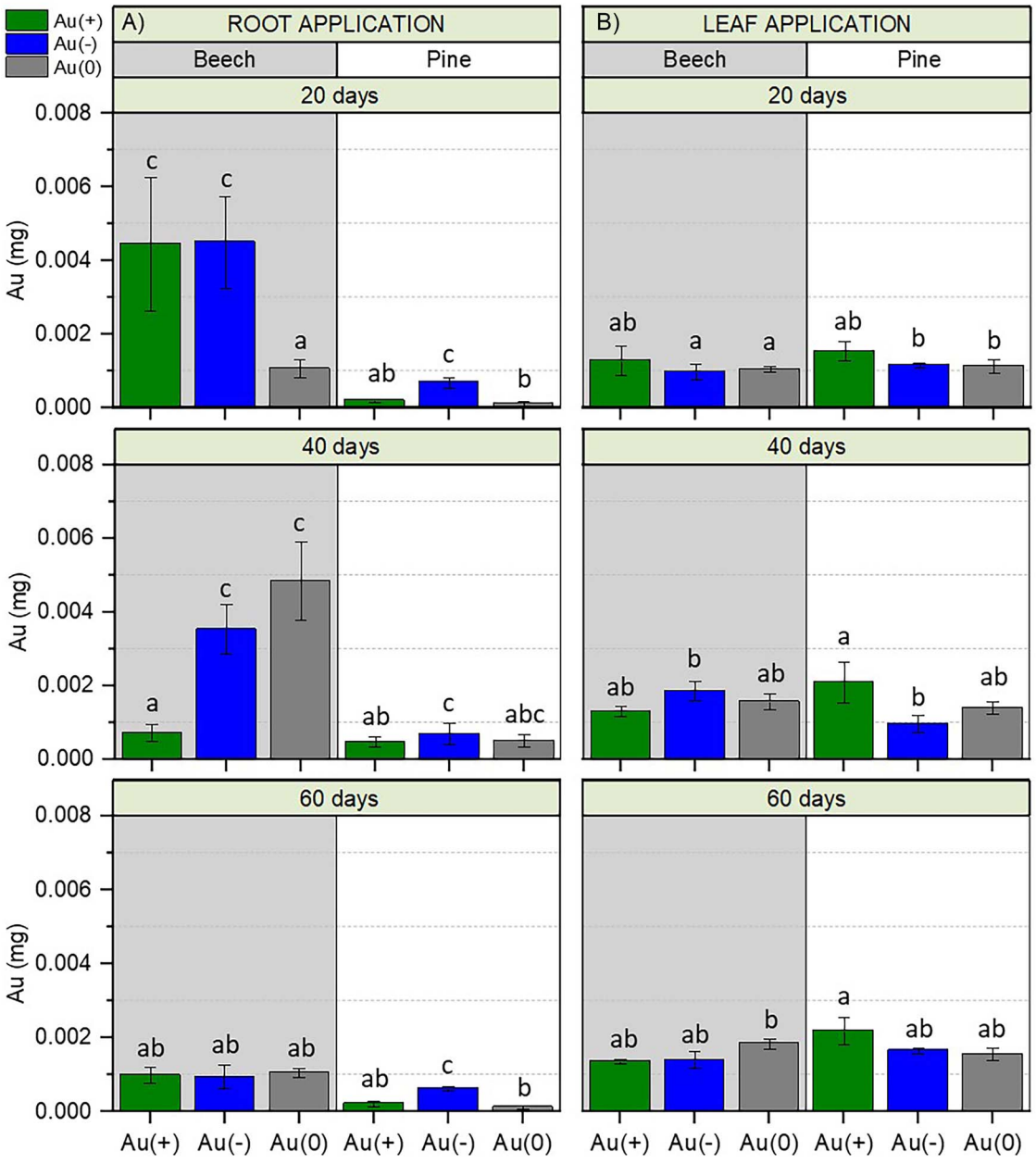

Figure 3. Amount of gold (mg) in (A) fine roots (root application) and (B) leaves (leaf application) at 20, 40 and 60 days after the Au-NP treatments. Data show the means ± SE (n = 3). Different letters stand for statistical differences between time and Au-NP treatment groups within a species at $P < 0.05$.

Leaf application Gold was detected in high concentrations in the leaves and low concentrations in the stem and in the roots in beech and pine after Au-NP application on the leaves (Figure 2B). The Au-NPs detected in the leaves could be temporarily stored in the mesophyll structure before eventually reaching the conductive systems (i.e., phloem and xylem). The combination of 2D chemical imaging and 3D chemical tomography revealed that a large number of Au-NPs were still adhering to the surface of a beech leaf even after washing (Figure 5 and 6; see Video S1 available as Supplementary data at *Tree Physiology* Online), which could also be the case for the pine needles. Although Avellan et al. (2019) reported that Au-NPs of large sizes (50 nm) are washed off very easily, and only few Au-NPs were detected on the leaf of wheat, hydrophobic epicuticular waxes and epicuticular hairs (i.e., trichomes) in pine and beech, respectively, could trap the majority of Au-NPs on the foliar surface, preventing the particles to penetrate inside the leaf. As observed in the 2D XRF images, Au-NPs were abundantly associated with the trichomes, clearly visible on those attached to the petiole and along the midrib (Figure 5A, and C). Similarly, an accumulation of Au-NPs was observed on the bases of trichomes in wheat after foliar exposure (Avellan et al. 2019).

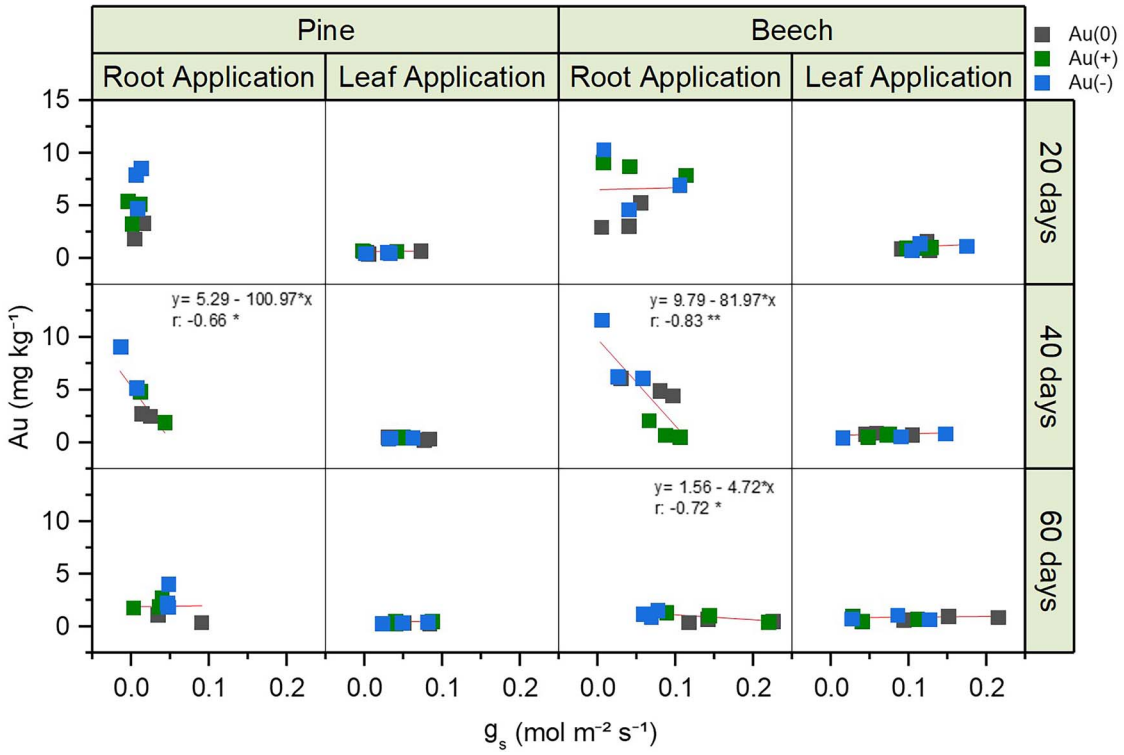

Figure 4. Relation between the stomatal conductance (g_s) and the Au concentration in leaves and roots (for leaf and root application, respectively) at 20, 40 and 60 days after Au-NP application (n = 9). Significant correlations are indicated: '**' $P < 0.01$, '*' $P < 0.05$.

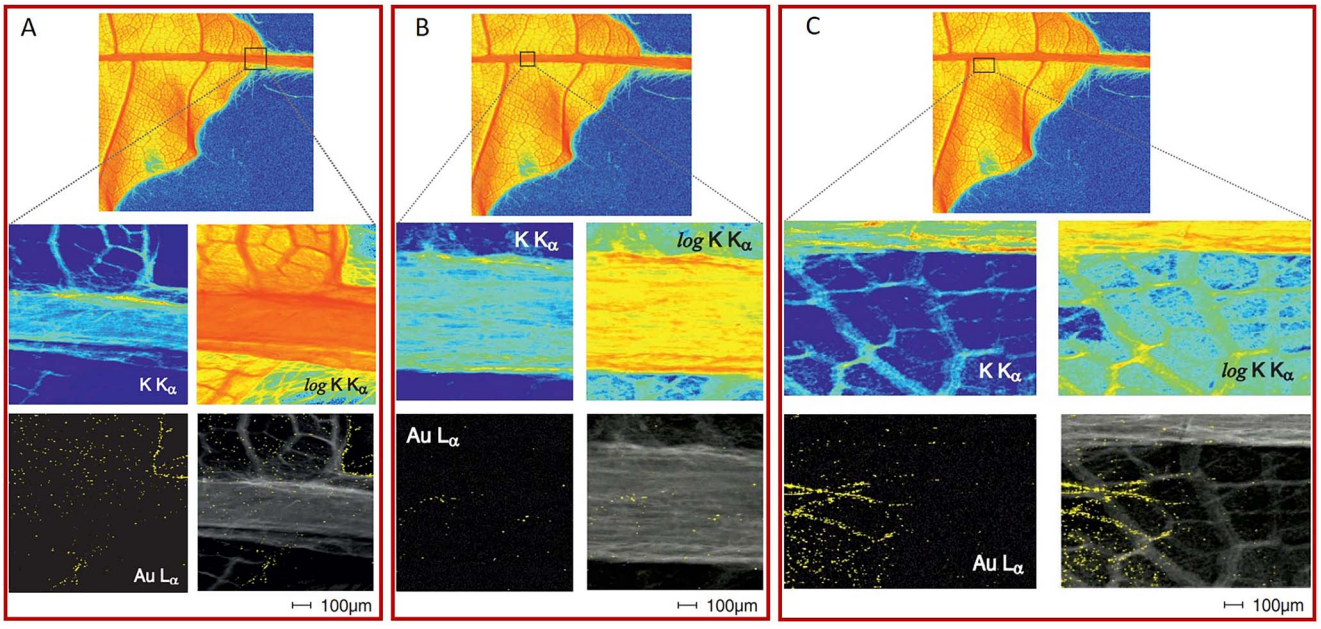

Figure 5. 2D XRF scanning images of leaf and petiole of beech exposed to Au-NPs (here Au(−) NPs). The contour and structure of the leaf and petiole are indicated by local K distribution and concentration given in log scale. The yellow spots indicate Au in particulate form along (A) the petiole, (B) the midrib and (C) in proximity of lateral veins. Scale bars 100 μm.

Foliar trichomes demonstrated to be a major driver of foliar water uptake (FWU) in beech because of strong hygroscopic properties conferred by their structural and chemical design (Schreel et al. 2020). To assess the contribution to FWU by trichomes, Schreel et al. (2020) applied Ag nitrate ionic tracer on the ad- and abaxial leaf surface in beech and observed

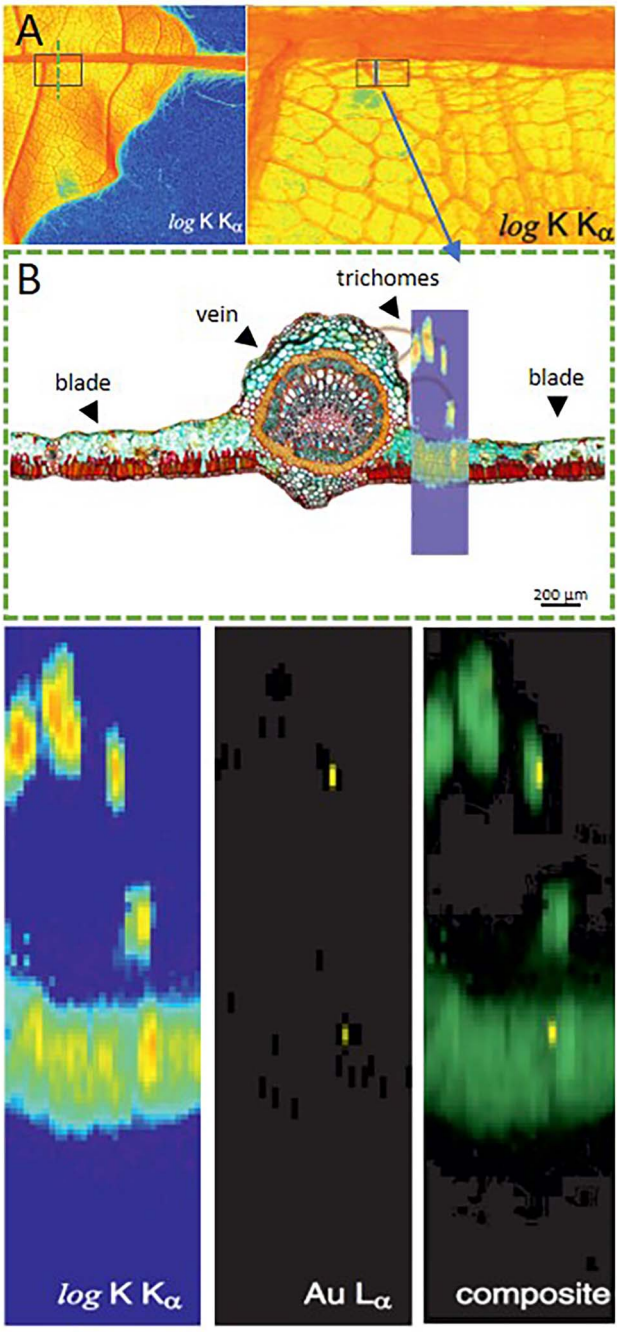

Figure 6. Chemical tomography of an undisturbed sub-volume in the proximity of lateral veins of the beech leaf. The 3D chemical information is obtained by confocal X-ray microscopy. Location of the sub-volume potentially containing Au-NPs (lower side of the leaf) is selected based on hierarchical 2D chemical analysis (A). The location of the tomographic volume is indicated by the square (right side of A). (B) Schematic representation of a section of a beech leaf indicating the position of the tomographic slice shown in the bottom panels. The cross section of the leaf blade and of several trichomes are detected based on the spatial distribution of potassium (log scale). Two isolated Au-NPs are observed. The composite image clearly indicates one Au-NP in the leaf blade and one inside/on a trichome. Schematic illustration of beech leaf cross section modified from Schreel et al. (2020), *The Plant Journal* (Copyright 2020 by Willey and Sons).

that Ag-NPs were abundantly present in the subepidermal cells of the midveins, after entering the leaf via trichomes as Ag^+ ions and then precipitating as Ag-NPs. Although the majority of Au-NPs were adhering to the surface of the trichomes, 3D confocal imaging provided evidence for an isolated Au-NP potentially inside a trichome (indicated by K distribution) and another isolated Au-NP clearly visible about 20–30 μm below the leaf surface (Figure 6B). We thus hypothesize two possible pathways of foliar uptake: first, most of the Au-NPs in beech and pine penetrated in the leaves primarily through stomatal pathways (as documented by the majority of studies; e.g., Eichert et al. 2008, Räsänen et al. 2017, Ha et al. 2021), and second, trichomes of beech leaves were partially involved in the uptake and downward transport of NPs along with water or immobilized the NPs after stomatal uptake as a depuration process before eventually exuding them (Avellan et al. 2021). To date, however, the role of trichomes in the NPs immobilization or uptake is not yet clear (Schwab et al. 2016). Although it is known that the number and size of stomata contributing to the NP uptake are highly variable among plant species and not all stomata are penetrated (Eichert et al. 2008), our results showed that Au content generally increased over time probably due to a continuous but slow diffusion of Au-NPs in the stomata while also the leaf biomass was increasing (Figure 3B). Once taken up, NPs can enter plant cells via several possible pathways such as binding to carrier proteins, through aquaporins, ion channels, endocytosis or binding to organic chemicals (Schwab et al. 2016). Once inside the cells, NPs were found in cell membranes, cytoplasm, mitochondria, chloroplasts and other organelles (Zhai et al. 2014). Ma and Quah (2016) observed that Au-NPs with different surface charge showed different internalization locations: uncoated, neutral and negative Au-NPs were attached to the nucleus, in vesicles and mitochondria, respectively.

Beech trees were able to take up and transport more Au than pine (Figure 2). Higher foliar penetration of NPs can be linked to higher stomatal density in beech (420 mm^{-2}; Van Wittenberghe et al. 2012) than in pine (46 mm^{-2} on adaxial side, 65 mm^{-2} on abaxial side; Lin et al. 2001). Although the stomatal size in coniferous species is generally higher than in broad-leaved species (Li et al. 2021), the presence of epicuticular wax in pine could trap the Au-NPs on the needle surface and prevent their internalization (Schwab et al. 2016).

A small fraction of Au was found in the stem, probably transported via phloem. The Au-NPs must have passed through the petiole, an important plant organ that connects stems with leaves and is involved in the transport of water, nutrients and biochemical signals. An even distribution of Au-NPs can be observed on the surface or inside the tissues of the petiole (Figure 5A). As suggested by Cocozza et al. (2019), the phloem transport of NPs from leaves to the stem along with photosynthates is possible in trees. Although the uptake mechanisms are not yet clear, aqueous apoplastic movement through

the cell walls and into the phloem after foliar penetration of NPs was revealed in citrus leaves (Etxeberria et al. 2016). Au-NPs in the roots were only detected in the Au(−) treatment in beech and in the Au(+) treatment in pine. These results could be explained by Au concentration below the detection limit or by root-to-soil exudation of NPs bound to phloem metabolites. In fact, in Avellan et al. (2019), Au-NPs were detected in the rhizosphere soil adhering to the roots of wheat, indicating that leaf-to-rhizosphere transport is possible, regardless of the surface coatings.

Gold in the stem: root vs leaf application Transport of Au-NPs to other organs seems to be more efficient after leaf application than after root application, as Au was detected in the roots of leaf application but not in the leaves of the root application (Figure 2B and A, respectively). In fact, it has been reported that foliar applications can result in larger amounts of NPs into plants compared with root applications (Su et al. 2020). The leaf uptake and transport of Au-NPs was species-specific, which can be linked to differences in the leaf characteristics (e.g., presence of trichomes or wax), stomatal density and size, the wood characteristics and the average phloem transport speed (as documented higher in angiosperms compared with gymnosperms; Liesche et al. 2015).

The detection of Au in the stem is supporting the uptake and transport in both ways, i.e., leaf-to-root and root-to-leaf, by both tree species. However, the Au concentration in the stem of beech was higher in the leaf than in the root application, whereas no differences were observed in pine. Our results are comparable to those reported by Cocozza et al. (2019), where the concentration of Ag in the stem was higher in the foliar than in the root treatment, and in poplar more than in oak and pine. The anatomy of the conductive vessels plays an important role in the NP transport, as well as the tree species, because of the species-specific wood anatomical structure in relation to the uptake and transport of NPs (Ballikaya et al. 2022). Pits in xylem were found to be larger in roots than in stems in *Picea* spp. (Schulte et al. 2015) and their size to vary from earlywood to latewood and with the age of cambium in conifer species (Sirviö and Kärenlampi, 1998). These features may suggest a reduced (in our case below the DL) or no transport of NPs in pine from the roots to the leaves and an accumulation of some NPs in the tracheids of the xylem having their transport restricted by the pit membranes (Corredor et al. 2009). Pits in various angiosperm species showed sizes below 50 nm (Zhang et al. 2020), which could explain lower Au concentrations in the stem of beech after root uptake than after leaf uptake. In contrast, in the phloem, large diameters (from 1.2 up to 7 μm and 0.3 to 0.6 μm in angiosperms and gymnosperms, respectively) of the sieve pores could transport NPs for longer distances through the phloem after leaf uptake (Ballikaya et al. 2022), as confirmed by Au detected in the roots of some leaf-treated trees.

Role of the surface charge and the stomatal conductance on the Au-NP uptake and transport

Influence of the surface charge In the leaf application 20 days after the treatments, Au(−) NPs in beech were found in the stem and in the roots, suggesting that Au-NPs with the lowest zeta potentials are more likely to be transported from the leaves to the roots, as also reported by Avellan et al. (2019). However, Au(+) NPs in pine were also found in the roots, indicating that the transport of NPs can be influenced by other unknown driving factors, which could be linked to the wood characteristic as previously discussed. In the root application 20 days after the treatments, Au(−) NPs accumulated in roots of pine to the highest extent which could mean that the negative charges on the Au-NP surface did not prevent interactions with the roots, whose surface and mucilage are also likely to be negatively charged (Zhu et al. 2012). A different trend was observed in beech, where Au(+) and Au(−) NPs accumulated to a similar degree, probably due to differences that are plant-species dependent (e.g., trichomes or higher stomatal density in beech could have trapped or taken up more Au-NPs than in pine, independently of the surface charge). Au(0) NPs in both species had the lowest concentration, probably because of their relatively more hydrophobic coating that increased their interaction with the root surface in the hydroponic solution. Moreover, DLS measurements (Table S1 available as Supplementary data at *Tree Physiology* Online) suggested an agglomeration of the Au-NPs, particularly strong for the Au(−) NPs, in Hoagland's solution which could have had a major impact on their uptake and transport. However, it is important to remember that in complex soil systems, the relationship between NP charge and root uptake can be more complicated.

In comparing our data with previous studies involving the influence of the surface charge on the uptake and transport of NPs in annual plants, we found that the influence of the surface charge did not show a clear trend in the examined tree species. The relationship between Au-NP surface charge and root uptake has been demonstrated to affect the uptake and transport of NPs (Zhu et al. 2012, Ma and Quah, 2016, Li et al. 2016), but it was shown that Au-NP transport from shoots to roots was not affected by different surface coatings (Avellan et al. 2019). Considering this, the surface charge of the Au-NPs could have played a role in the adsorption and uptake of the Au-NPs by roots and leaves, but not in their transport to different plant compartments as no significant differences were found among treatments in the Au detected in the stem. One reason could be that Au-NP surfaces can acquire additional organic coatings (so called organic corona), such as proteins lipids and carbohydrates, present in the phloem or xylem which may have effects on the NP aggregation, cellular uptake and transport (Avellan et al. 2019).

Influence of the stomatal conductance of Au-NP root-treated trees In the root application treatment, when the stomatal conductance (g_s) increased, the Au concentration decreased significantly, and it can be seen in both species at 40 and 60 days after the experiment (Figure 4). This interaction was not significant at 20 days, closer to the application time. It is likely that the stomatal activity did not influence the root uptake of Au-NPs, as well as the leaf uptake since no correlation was found. Instead, we propose three hypotheses that could explain the negative correlation between stomatal conductance and Au concentration:

(i) Higher g_s is known to occur when root growth is enhanced as a result of increased demand for water. Since the Au concentration in the roots decreased over time mostly due to increased plant biomass (dilution effect), the negative correlation with increasing g_s at 40 and 60 days was more likely to reflect this aspect.

(ii) Increasing g_s could have caused the allocation of Au, transported upwards with water and nutrients from the roots to different parts of the trees. Results from Lintern et al. (2013) showed that gold from buried gold deposits can be exuded or compartmentalized by the leaves at high concentrations, probably toxic to plants (in this case to *Eucalyptus* trees). However, we have no evidence of Au efflux through leaf exudates or compartmentalization in the leaves of Au-treated trees.

(iii) Increased g_s in the root-treated trees may have contributed to the exudation of Au from the roots into the soil together with primary metabolites (e.g., sugars, amino acids and organic acids) due to the close coupling between photosynthetic activity and root exudation (Canarini et al. 2019). Root exudation is a complex phenomenon that is involved in the transport of metabolites through plasmodesmata from the phloem to the actively growing root tip where metabolites are exuded into the soil by diffusion processes and specific efflux carriers and channels (Canarini et al. 2019). Root exudates can modify the solubility, sorption and transport of mineral elements to the roots, thus influencing nutrient availability in the soil and interacting with symbiotic microorganisms (Kuzyakov et al. 2003). Forty and 60 days after the treatment, the trees might have released more root exudates due to higher nutrient demand, triggering the exudation of Au-NPs, which are probably bound to primary metabolites. Similar hypothesis was discussed by Avellan et al. (2019) in wheat, where Au-NPs were transported from the leaves and exudated into the surrounding soil through the roots. Exudation of Ag-NPs in citrus trees through the root hairs into the soil was also reported, as high amount of Ag was found in the roots (Su et al. 2020).

Our results did not show any correlation between g_s and Au concentration after leaf uptake, although it has been reported that increase in transpiration rate and stomatal conductance resulted in high intercellular concentration of volatile organic compounds in ornamental plants (Dela Cruz et al. 2014). Thus, in our experiments, Au-NP leaf uptake could be mostly related to the species-specific stomatal density and size rather than to gas exchange, as previously discussed.

Conclusions

Our study shows that trees are able to effectively take up Au-NPs and transport them through the plant system, following species-specific mechanisms of interaction, which are associated with physical and physiological factors. The surface charge of the Au-NPs could have played a role in the adsorption and uptake of the Au-NPs by roots and leaves, but not in their transport to different plant compartments. These results raise questions about the role of surface charge on the uptake and transport of NPs in woody species when compared with previous studies with NP coating surfaces and annual plants. The negative correlation between stomatal conductance and Au concentration might be linked to root exudation of Au, its upward allocation to higher compartments of the tree, such as leaves, or increased biomass and dilution effect.

Although there are still many open questions that need additional work for a complete understanding, we showed the first evidence of gold NP uptake and transport in beech and in pine, which contributes to a better understanding of the interactions of NPs with different tree species.

Conflict of interest

None declared.

Authors' contributions

P.B., C.C., I.B. and P.C. planned and designed the study. P.B., I.B., D.G., C.C., M.E.M., B.S. and P.C. performed experiments and conducted fieldwork. P.B, C.C., D.G., R.K., M.S., L.S., B.S. and P.C. analyzed and interpreted the data. P.B., D.G. and P.C. wrote the manuscript. All authors contributed to writing and editing the manuscript.

Supplementary data

Supplementary data for this article are available at *Tree Physiology* Online.

Acknowledgments

We are sincerely grateful for the technical support and advice given by Loïc Schneider, Daniele Pezzotta and Beat Stierli; Claudio Cattaneo and Gabor Reiss for the greenhouse and plants organization; and Luc Schnell, Nadja Studer, Dr Nasrullah Khan, Ariane Dieth and Nicola Umiker for their practical help during the plant harvesting and biomass weighting (WSL, Birmensdorf,

Switzerland). We especially acknowledge the Paul Scherrer Institut (Villigen, Switzerland) for provision of synchrotron radiation beamtime at the beamline microXAS, and thank M. Birri, B. Meyer and D. Ferreira Sanchez for technical assistance and scientific discussions.

Funding

The work was supported by the Swiss National Science Foundation (SNSF, Beitragsnummer SNF: 200021_182042). L.S. was supported by SNF P500PB_203127.

References

Arora S, Sharma P, Kumar S, Nayan R, Khanna PK, Zaidi MGH (2012) Gold-nanoparticle induced enhancement in growth and seed yield of *Brassica juncea*. Plant Growth Regul 66:303–310.

Avellan A, Simonin M, McGivney E et al. (2018) Gold nanoparticle biodissolution by a freshwater macrophyte and its associated microbiome. Nat Nanotechnol 13:1072–1077.

Avellan A, Yun J, Zhang Y et al. (2019) Nanoparticle size and coating chemistry control foliar uptake pathways, translocation, and leaf-to-rhizosphere transport in wheat. ACS Nano 13:5291–5305.

Avellan A, Yun J, Morais BP, Clement ET, Rodrigues SM, Lowry GV (2021) Critical review: role of inorganic nanoparticle properties on their foliar uptake and in planta translocation. Environ Sci Technol 55:13417–13431.

Ballikaya P, Marshall J, Cherubini P (2022) Can tree-ring chemistry be used to monitor atmospheric nanoparticle contamination over time? Atmos Environ 268:118781. https://doi.org/10.1016/j.atmosenv.2021.118781.

Canarini A, Kaiser C, Merchant A, Richter A, Wanek W (2019) Root exudation of primary metabolites: mechanisms and their roles in plant responses to environmental stimuli. Front Plant Sci 10:157.

Cocozza C, Perone A, Giordano C, et al. (2019) Silver nanoparticles enter the tree stem faster through leaves than through roots. Tree Physiol 39:1251–1261.

Corredor E, Testillano PS, Coronado MJ et al. (2009) Nanoparticle penetration and transport in living pumpkin plants: in situ subcellular identification. BMC Plant Biol 9:1–11.

Dela Cruz M, Christensen JH, Thomsen JD, Muller R (2014) Can ornamental potted plants remove volatile organic compounds from indoor air? A review. Environ Sci Pollut Res 21:13909–13928.

Du W, Tan W, Peralta-Videa JR, Gardea-Torresdey JL, Ji R, Yin Y, Guo H (2017) Interaction of metal oxide nanoparticles with higher terrestrial plants: physiological and biochemical aspects. Plant Physiol Biochem 110:210–225.

Eichert T, Kurtz A, Steiner U, Goldbach HE (2008) Size exclusion limits and lateral heterogeneity of the stomatal foliar uptake pathway for aqueous solutes and water-suspended nanoparticles. Physiol Plant 134:151–160.

Etxeberria E, Gonzalez P, Bhattacharya P, Sharma P, Ke PC (2016) Determining the size exclusion for nanoparticles in citrus leaves. HortScience 51:732–737.

Feichtmeier NS, Walther P, Leopold K (2015) Uptake, effects, and regeneration of barley plants exposed to gold nanoparticles. Environ Sci Pollut Res 22:8549–8558.

Ha N, Seo E, Kim S, Lee SJ (2021) Adsorption of nanoparticles suspended in a drop on a leaf surface of *Perilla frutescens* and their infiltration through stomatal pathway. Sci Rep 11:1–13.

Han D, Shen H, Duan W, Chen L (2020) A review on particulate matter removal capacity by urban forests at different scales. Urban For Urban Green 48:126565. https://doi.org/10.1016/j.ufug.2019.126565.

Hoagland DR, Arnon DI (1950) The water-culture method for growing plants without soil. Circular. California agricultural experiment station 347: 2nd edn, pp. 32.

Hong J, Peralta-Videa JR, Rico C, Sahi S, Viveros MN, Bartonjo J, Zhao L, Gardea-Torresdey JL (2014) Evidence of translocation and physiological impacts of foliar applied CeO_2 nanoparticles on cucumber (*Cucumis sativus*) plants. Environ Sci Technol 48:4376–4385.

Judy JD, Unrine JM, Rao W, Wirick S, Bertsch PM (2012) Bioavailability of gold nanomaterials to plants: importance of particle size and surface coating. Environ Sci Technol 46:8467–8474.

Khan MN, Mobin M, Abbas ZK, AlMutairi KA, Siddiqui ZH (2017) Role of nanomaterials in plants under challenging environments. Plant Physiol Biochem 110:194–209.

Koelmel J, Leland T, Wang H, Amarasiriwardena D, Xing B (2013) Investigation of gold nanoparticles uptake and their tissue level distribution in rice plants by laser ablation-inductively coupled-mass spectrometry. Environ Pollut 174:222–228.

Kranjc E, Mazej D, Regvar M, Drobne D, Remškar M (2018) Foliar surface free energy affects platinum nanoparticle adhesion, uptake, and translocation from leaves to roots in arugula and escarole. Environ Sci Nano 5:520–532.

Kumar N, Tripathi P, Nara S (2018) Gold nanomaterials to plants: impact of bioavailability, particle size, and surface coating. In: Nanomaterials in plants, algae, and microorganisms. Academic Press, Elsevier, London, pp 195–220.

Kuzyakov Y, Raskatov A, Kaupenjohann M (2003) Turnover and distribution of root exudates of *Zea mays*. Plant Soil 254: 317–327.

Larue C, Castillo-Michel H, Sobanska S, Cécillon L, Bureau S, Barthès V, Ouerdane L, Carrière M, Sarret G (2014) Foliar exposure of the crop Lactuca sativa to silver nanoparticles: evidence for internalization and changes in Ag speciation. J Hazard Mater 264:98–106.

Li H, Ye X, Guo X, Geng Z, Wang G (2016) Effects of surface ligands on the uptake and transport of gold nanoparticles in rice and tomato. J Hazard Mater 314:188–196.

Li L, Luo Y, Li R, Zhou Q, Peijnenburg WJ, Yin N, Yang J, Tu C, Zhang Y (2020) Effective uptake of submicrometre plastics by crop plants via a crack-entry mode. Nat Sustain 3:929–937.

Li Q, Hou J, He N, Xu L, Zhang Z (2021) Changes in leaf stomatal traits of different aged temperate forest stands. For Res 32:927–936.

Liesche J, Windt C, Bohr T, Schulz A, Jensen KH (2015) Slower phloem transport in gymnosperm trees can be attributed to higher sieve element resistance. Tree Physiol 35:376–386.

Lin J, Jach ME, Ceulemans R (2001) Stomatal density and needle anatomy of Scots pine (*Pinus sylvestris*) are affected by elevated CO_2. New Phytol 150:665–674.

Lintern M, Anand R, Ryan C, Paterson D (2013) Natural gold particles in Eucalyptus leaves and their relevance to exploration for buried gold deposits. Nat Commun 4:2614.

Liu W, Zeb A, Lian J, Wu J, Xiong H, Tang J, Zheng S (2020) Interactions of metal-based nanoparticles (MBNPs) and metal-oxide nanoparticles (MONPs) with crop plants: a critical review of research progress and prospects. Environ Rev 28:294–310.

Luo X, Cao J (2018) Discovery of nano-sized gold particles in natural plant tissues. Environ Chem Lett 16:1441–1448.

Lv J, Christie P, Zhang S (2019) Uptake, translocation, and transformation of metal-based nanoparticles in plants: recent advances and methodological challenges. Environ Sci Nano 6:41–59.

Ma X, Quah B (2016) Effects of surface charge on the fate and phytotoxicity of gold nanoparticles to phaseolus vulgaris. J Food Chem Nanotechnol 2:57–65.

Ma X, Yan J (2018) Plant uptake and accumulation of engineered metallic nanoparticles from lab to field conditions. Curr Opin in Environmental Sci Health 6:16–20.

Ma X, Geiser-Lee J, Deng Y, Kolmakov A (2010) Interactions between engineered nanoparticles (ENPs) and plants: phytotoxicity, uptake and accumulation. Sci Total Environ 408:3053–3061.

Murazzi ME, Cherubini P, Brunner I et al. (2022) Can forest trees take up and transport nanoplastics? iForest 15:128.

Räsänen JV, Leskinen JT, Holopainen T, Joutsensaari J, Pasanen P, Kivimäenpää M (2017) Titanium dioxide (TiO_2) fine particle capture and BVOC emissions of *Betula pendula* and *Betula pubescens* at different wind speeds. Atmos Environ 152:345–353.

Renninger HJ, Carlo NJ, Clark KL, Schäfer KV (2015) Resource use and efficiency, and stomatal responses to environmental drivers of oak and pine species in an Atlantic Coastal Plain forest. Front Plant Sci 6:297.

Schreel JD, Leroux O, Goossens W, Brodersen C, Rubinstein A, Steppe K (2020) Identifying the pathways for foliar water uptake in beech (*Fagus sylvatica* L.): a major role for trichomes. Plant J 103:769–780.

Schulte PJ, Hacke UG, Schoonmaker AL (2015) Pit membrane structure is highly variable and accounts for a major resistance to water flow through tracheid pits in stems and roots of two boreal conifer species. New Phytol 208:102–113.

Schwab F, Zhai G, Kern M, Turner A, Schnoor JL, Wiesner MR (2016) Barriers, pathways and processes for uptake, translocation and accumulation of nanomaterials in plants–Critical review. Nanotoxicology 10:257–278.

Serrano L, Gamon JA, Berry J (1997) Estimation of leaf area with an integrating sphere. Tree Physiol 17:571–576.

Siddiqi KS, Husen A (2016) Engineered gold nanoparticles and plant adaptation potential. Nanoscale Res Lett 11:1–10.

Sirviö J, Kärenlampi P (1998) Pits as natural irregularities in softwood fibers. Wood Fiber Sci 30:27–39.

Solé VA, Papillon E, Cotte M, Walter P, Susini JA (2007) A multiplatform code for the analysis of energy-dispersive X-ray fluorescence spectra. Spectrochimica Acta Part B: At Spectrosc 62:63–68.

Su Y, Ashworth V, Kim C, Adeleye AS, Rolshausen P, Roper C, White J, Jassby D (2019) Delivery, uptake, fate, and transport of engineered nanoparticles in plants: a critical review and data analysis. Environ Sci Nano 6:2311–2331.

Su Y, Ashworth VE, Geitner NK, Wiesner MR, Ginnan N, Rolshausen P, Roper C, Jassby D (2020) Delivery, fate, and mobility of silver nanoparticles in citrus trees. ACS Nano 14:2966–2981.

Taylor AF, Rylott EL, Anderson CW, Bruce NC (2014) Investigating the toxicity, uptake, nanoparticle formation and genetic response of plants to gold. PLOS one 9:e93793.

Tripathi DK, Singh S, Singh S, Pandey R, Singh VP, Sharma NC, Prasad SM, Dubey NK, Chauhan DK (2017) An overview on manufactured nanoparticles in plants: uptake, translocation, accumulation and phytotoxicity. Plant Physiol Biochem 110:2–12.

Uzu G, Sobanska S, Sarret G, Munoz M, Dumat C (2010) Foliar lead uptake by lettuce exposed to atmospheric fallouts. Environ Sci Technol 44:1036–1042.

Van Wittenberghe S, Adriaenssens S, Staelens J, Verheyen K, Samson R (2012) Variability of stomatal conductance, leaf anatomy, and seasonal leaf wettability of young and adult European beech leaves along a vertical canopy gradient. Trees 26:1427–1438.

Wojcieszek J, Jiménez-Lamana J, Ruzik L, Asztemborska M, Jarosz M, Szpunar J (2020) Characterization of TiO2 NPs in radish (*Raphanus sativus* L.) by single-particle ICP-QQQ-MS. Frontiers in Environmental Science 8:100.

Zhai G, Walters KS, Peate DW, Alvarez PJ, Schnoor JL (2014) Transport of gold nanoparticles through plasmodesmata and precipitation of gold ions in woody poplar. Environ Sci Technol Lett 1:146–151.

Zhang Y, Carmesin C, Kaack L et al. (2020) High porosity with tiny pore constrictions and unbending pathways characterize the 3D structure of intervessel pit membranes in angiosperm xylem. Plant Cell Environ 43:116–130.

Zhu ZJ, Wang H, Yan B, Zheng H, Jiang Y, Miranda OR, Rotello VM, Xing B, Vachet RW (2012) Effect of surface charge on the uptake and distribution of gold nanoparticles in four plant species. Environ Sci Technol 46:12391–12398.